ELSEVIER

Journal of Molecular Catalysis A: Chemical 162 (2000) 381–390

JOURNAL OF MOLECULAR CATALYSIS A: CHEMICAL

www.elsevier.com/locate/molcata

^{51}V and ^{31}P NMR studies of VO_x/TiO_2 catalysts modified by phosphorous

O.B. Lapina*, D.F. Khabibulin, A.A. Shubin, V.M. Bondareva

Boreskov Institute of Catalysis, Pr. Lavrentieva 5, 630090, Novosibirsk, Russia

Abstract

Phosphorous-doped VO_x/TiO_2 catalysts prepared by the spray-drying method and treated under catalytic reaction, as well as individual phases (α_I-, α_{II}-, β-) of $VOPO_4$ were studied using modern high-resolution solid-state NMR techniques, including fast magic angle spinning (MAS), combined with the analysis of rotational satellites intensities by the satellite transition spectroscopy (SATRAS) method; 2D triple-quantum, quintuple-quantum MAS NMR, and spin mapping echo experiments. The simultaneous determination of chemical shielding anisotropy and quadrupole tensor parameters, as well as their distributions, permits to draw a conclusion on the local environment of vanadium sites in the catalysts. The formation of a triple V–P–Ti compound in phosphorous-doped VO_x/TiO_2 catalysts has been revealed. Only one type of slightly distorted tetrahedral vanadium atoms bound via oxygen to phosphorous was found in this compound. The very large distribution of the quadropole constant points to the irregular structure of this compound.

Keywords: Vanadium; Phosphorous; Titanium oxide; Solid-state; NMR; SATRAS; MQMAS; Spin mapping echo

1. Introduction

VO_x/TiO_2 catalysts used in industry (reviews in Refs. [1,2] and references therein) usually contain various additives, and among them, phosphorous is one of the main. Nevertheless, the influence of the phosphorous on the structure of the catalysts is not obvious. Only few publications are devoted to the study of VO_x/TiO_2 catalysts promoted by phosphorous [3–9]. Soria et al. [3] noticed the interaction of phosphoric acid, not only with the vanadium species deposited on the outer part of the titania support, but also with the surface TiO_2 layers. The resulting vanadium and titanium phosphates were found to be strongly influenced by the phosphorous content. Deo and Wachs [4] have found by X-Ray diffraction (XRD) that the effect of P_2O_5 on the surface vanadium oxide phase depends on the concentration and sequence of preparation. Upon addition of higher concentrations of P_2O_5 (when the P/V ratio in the catalysts is greater than 1.25), vanadium phosphate compound (α_I-$VOPO_4$) is formed, which appears to have vanadium–oxygen–phosphorous bonds with the surface phosphorous oxide phase. Whereas, the addition of 1% V_2O_5 to a 5% P_2O_5/TiO_2 does not show any evidence of vanadium phosphate compound formation. The changing of the sequence of impregnation of phosphorous and vanadia on titania suggests that phosphorous oxide does not discriminate be-

* Corresponding author.
E-mail address: olga@catalysis.nsk.su (O.B. Lapina).

1381-1169/00/$ - see front matter
PII: S1381-1169(00)00305-8

tween the TiO_2 surface, or the surface of vanadium oxide phase interacts strongly with both of them. Hengstum et al. [5] have concluded, from the results of the catalytic oxidation experiments, that the addition of phosphorous resulted in an increase of the surface acidity of VO_x/TiO_2 catalysts. Alyea et al. [6] have found that phosphate addition to the titania support, prior to vanadia addition, resulted in the formation of only octahedrally coordinated vanadia species and slightly decreased the interaction between vanadia and titania. Overbeek et al. [7] have concluded that the oxide phase is amorphous and very well dispersed over the surface of the support in the case of titania-supported vanadium–phosphorous oxide catalysts prepared via deposition–precipitation from a homogeneous solution of low valent vanadium ions in combination with phosphate-ions onto titania support bodies. It was also found that the active phase exhibits a very strong interaction with the titania support. Spectroscopy data for V_2O_5/TiO_2 catalysts, modified by different amounts of P_2O_5 (P/V ratios of 0–3.3) prepared by impregnation in the presence of oxalic acid, showed that the addition of P_2O_5 favours the formation of supported vanadyl phosphate and isolated V^{4+} species [8]. EXAFS analysis of titania-supported V–P–O catalysts ($\sim$8 wt.% V), prepared by means of homogeneous deposition–precipitation, revealed structural differences between the V–P–O phases in these catalysts and bulk V–P–O catalysts. It was also found that vanadyl phosphate is not the active phase in this reaction [9].

It is clearly seen that the method of catalysts preparation, relative concentrations of vanadium and phosphorous, and the procedure of the additive introduction, should be critical. Nevertheless, even for the catalysts prepared by similar ways, there are some discrepancies in the determined structures. In the present study, the influence of phosphorous addition on the structural properties of VO_x/TiO_2 catalysts, prepared by the spray-drying method, was investigated by modern solid-state ^{31}P and ^{51}V NMR techniques.

Whereas ^{31}P NMR, which permits to distinguish the oxidation state of vanadium in the system [10–13] and discriminate between different $VOPO_4$ phases [11,13–17], nowadays is most practical in application to the study of vanadia–phosphorous systems, ^{51}V NMR became one of the most informative methods for the characterisation of the local environment of solid-state vanadia-based catalysts [18–23]. New NMR techniques permit one to extract precisely all the parameters of chemical shielding and the quadrupole tensors (including the relative orientation of tensors) that determined solid-state NMR line shape. Among these techniques are: satellite transition spectroscopy (SATRAS), which is the variant of high speed magic angle spinning (MAS) with the precise analysis of the intensity of spinning sidebands [24–29]; and high-resolution multiple quantum magic angle spinning (MQMAS) spectroscopy [30–39]. Under some suitable experimental conditions, these techniques may be used for the description of the local environment of the nuclei and its distortions.

2. Experimental

2.1. Sample preparation

$VOPO_4 \cdot 2H_2O$ was prepared as described in Refs. [40–42] by heating V_2O_5 with 85% H_3PO_4 (P/V = 7) under reflux for 16 h.

Pure $VOPO_4$ phases were prepared from $VOPO_4 \cdot 2H_2O$, according to [43]:

α_I-$VOPO_4$ — was obtained by dehydration of $VOPO_4 \cdot 2H_2O$ in dry air at 250°C,
α_{II}-$VOPO_4$ — was prepared from $VOPO_4 \cdot 2H_2O$ by dehydration in dry air at 720°C for 20 h, and
β-$VOPO_4$ — was obtained by heating of α_{II}-$VOPO_4$ at 800°C for 5 h.

The assignment of the phases formed in the course of the preparation and the purity of individual compounds was checked using powder XRD (Siemens D-500 diffractometer, monochromatised Cu K_α radiation).

The VO_x/TiO_2 catalysts, promoted by phosphorous (20 wt.% V_2O_5, 0–15 wt.% P_2O_5), were prepared by the spray-drying method, including the mixing of aqueous solutions of vanadyl oxalate, TiO_2 (anatase) and H_3PO_4, followed by subsequent drying and calcinations, as described in Ref. [44]. Before NMR measurements, catalysts were used

in the ammoxidation of methylpyrazine reaction (methylpyrazine/O_2/NH_3/H_2O = 1/8/17/17 (vol.%), the rest being N_2, at 250–350°C). The soluble surface compounds were extracted by washing in $2M \cdot HNO_3$ and water at ambient temperature with subsequent drying and calcination [18].

2.2. NMR measurements

NMR measurements were performed on Bruker MSL-400 and CXP-300 spectrometers in magnetic fields of 9.4 and 7.0 T, corresponding to a ^{51}V resonance frequency of 105.20 and 78.86 MHz and to a ^{31}P resonance frequency of 161.9 and 121.4 MHz, respectively. The ^{31}P and ^{51}V chemical shifts were referenced to external 85% H_3PO_4 and $VOCl_3$, respectively.

High-speed MAS ^{51}V and ^{31}P NMR spectra were recorded at rotation frequencies 10–15 kHz using 5 mm (outer diameter) Si_3N_4 rotors and the NMR probe from NMR Rotor Consult. (Denmark).

The ^{31}P spin echo mapping spectra [10–13] were recorded under static conditions, using a $90°x–\tau–180°y–\tau$ pulse sequence. The 90° pulse was 4.0 μs and τ was 20 μs. The irradiation frequency was varied in increments of 50 kHz.

Two-dimensional (2D) 3Q- and 5QMAS ^{51}V NMR spectra were recorded at ambient temperature. The standard acquisition scheme, consisting of preparation, evolution and detection periods, was used [30–32]. The length of the first 120° preparation pulse was 3.67 μs. Second refocusing pulse was 1.38 μs (45°) for 3QMAS experiments and 1.98 μs (65°) for 5QMAS experiments, respectively. The spectra were recorded with a recycle delay of 5 s. The phase of the first pulse was cycled in such a way to pick out the desirable multiple-quantum coherence. This pulse cycling was combined with a classic overall four-pulse cycle scheme, in order to minimize phase and amplitude receiver imperfections.

^{51}V NMR spectra parameters were determined from MAS rotational sidebands intensities using the SATRAS approach [24–29]. Simulations of both ^{51}V static and MAS NMR spectra were performed, taking into account the second-order quadrupole correction using the NMR5 program described earlier [45–47]. All simulations were performed on a dual PII-400 MHz CPU IBM PC compatible computer running Linux OS.

3. Results and discussion

According to the literature data [10–13], ^{31}P NMR spin echo mapping is a powerful technique to analyse the oxidation state of vanadium bound to phosphorous atoms. The signal at 2400 ppm is typical for phosphorous linked via oxygen to V^{4+} in $(VO)_2P_2O_7$. Similar signals are at 2300 ppm in $VO(H_2PO_4)_2$, at 1625 ppm in $VOHPO_4 \cdot 0.5H_2O$, and at 800 ppm in $VO(PO_3)_2$. The signal near 0 ppm is typical for phosphorous bound via oxygen to V^{5+} in $VOPO_4$ phases. The intermediate signal between 200–1200 ppm corresponds to phosphorous bound to both V^{4+} and V^{5+}. For VPO_4 (phase in the V^{3+} oxidation state), the ^{31}P NMR spin echo mapping signal is observed at 4600 ppm.

The ^{31}P NMR spin echo mapping spectra of VO_x/TiO_2 catalysts, promoted by phosphorous, represent a single line with chemical shift close to 0 ppm (Fig. 1A). According to the literature data, this indicates that practically all vanadium, bounded via oxygen to phosphorous, should have the oxidation state V^{5+} in these catalysts. These data are in agreement with ESR. According to these data, only 1–2% of vanadium in these catalysts is in the 4+ oxidation state. This is untypical for the binary V–P catalysts, in which the active phase is represented by a matrix of $(VO)_2P_2O_7$ with a low density of V^{5+} species on its surface, while in binary V–Ti catalysts, the main part of vanadium is V^{5+}.

A close examination of the ^{31}P NMR signal near 0 ppm by ^{31}P MAS allowed one to discriminate between the $VOPO_4$ phases in V–P systems [11,13–17]. In α_I-, α_{II}-, β-, δ- and γ-phases of $VOPO_4$, vanadium has the oxidation state 5+ and according to Abdelouahab et al. [15], only one signal at −20.5 ppm is observed in ^{31}P MAS for α_{II}-$VOPO_4$ and one signal at −11.5 ppm for β-$VOPO_4$, correspondingly. Only one line was detected in the ^{31}P MAS spectrum of α_I-$VOPO_4$ at 3.6 ppm [16]. The spectra of the δ-$VOPO_4$ and γ-$VOPO_4$ are more complex. γ-$VOPO_4$ shows two signals at −17.3 and −21.2 ppm with the same relative intensity and a shoulder

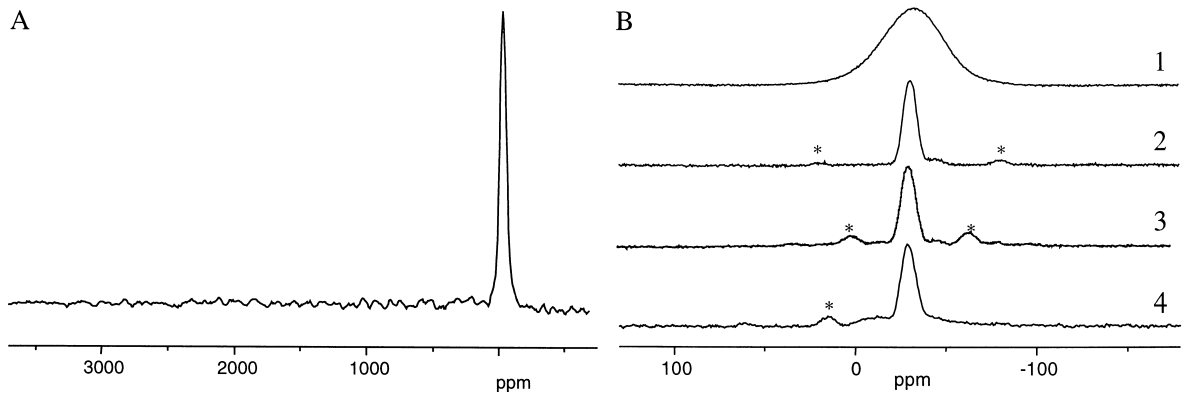

Fig. 1. (A) The ^{31}P spin echo mapping spectra of VO_x/TiO_2 catalyst containing 10 wt.% P_2O_5. (B) The ^{31}P MAS (spectra 1, 2, 3) and static (spectrum 4) spectra of VO_x/TiO_2 catalyst containing P_2O_5: 1 wt.% (spectrum 2) and 10 wt.% (spectra 3, 4). Spectrum 1 was obtained after the extraction procedure of the soluble vanadium from the spectrum 3. Spectra 1, 3 and 4 were obtained on 161.9 MHz, while spectrum 2 was obtained on 121.4 MHz. Rotational spinning sidebands are indicated by asterisks.

at -14.9 ppm. δ-$VOPO_4$ has two signals at -8.4 and -17.6 ppm and a weak peak around -6.5 ppm [15]. α_I-, α_{II}-, δ- and γ-phases of $VOPO_4$ can be easily hydrated. The $VOPO_4 \cdot 2H_2O$ dihydrate is the final product of hydration for all the phases. Its ^{31}P MAS spectrum has only one signal at 7.6 ppm [16].

^{31}P MAS spectra of VO_x/TiO_2 catalysts, promoted with different phosphorous concentrations, are shown in Fig. 1B. All the catalysts show a single peak at -30 ppm different from those for all (α_I-, α_{II}-, β-, δ-, γ-) $VOPO_4$ phases or their hydrated forms. Note that ^{31}P NMR signals from -20 to -40 ppm for the $VOPO_4$ catalysts, exposed under reaction conditions, was attributed by Vedrine et al. [17] to the interaction between $VOPO_4$ groups and $(VO)_2P_2O_7$. The absence of the latter phase in our system eliminates this possibility in our case. Thus, the observed ^{31}P signal at -30 ppm in VO_x/TiO_2 catalysts promoted by phosphorous could not be attributed to any $VOPO_4$ phases or their hydrates. The high-filed shift of this signal allows to propose that phosphorous in the catalysts is bound via oxygen, not only to vanadium (5+), but also to titanium atoms.

Combined ^{31}P NMR spin echo mapping and ^{31}P MAS data indicate that phosphorous in the promoted VO_x/TiO_2 catalysts is not bound to V^{4+} or V^{3+}, but only to V^{5+}, and, more probable, simultaneously to Ti^{4+}. Actually, the identification of the V^{5+} phases present in V–P catalysts by ^{31}P MAS NMR is difficult, due to their amorphous character, which, probably, could increase their ^{31}P NMR line width. To achieve a better characterisation of the catalysts, it is also necessary to examine their ^{51}V NMR spectra.

^{51}V static and MAS NMR spectra of VO_x/TiO_2 catalysts promoted by phosphorous with different phosphorous concentration are shown in Fig. 2. All the spectra represent the superposition of two lines: the line with axial anisotropy of the chemical shielding tensor ($\sigma_\perp = 310$ ppm, $\sigma_\parallel = 1270$ ppm) and the line with the maximum at -800 ppm. At low phosphorous concentrations, the line with the axial anisotropy of the chemical shielding tensor prevails in the spectra (Fig. 2A-1,2). The increase of the phosphorous content leads to the increase of the intensity of the line at -800 ppm (Fig. 2A-2,3,4), and with the phosphorous content close to 15wt.% of P_2O_5 (molar ratio of $V_2O_5/P_2O_5 \cong 1$), the latter line became the main in the spectrum (Fig. 2A-4). MAS NMR spectra of the same catalysts are shown in Fig. 2B. As could be seen, the line with axial anisotropy of chemical shielding tensor gives well-resolved spinning sidebands. The isotropic shift of this line (-612 ppm), its anisotropy, as well as all quadrupole tensors parameters for this spectrum, well coincide with those for V_2O_5 [24,27]. The line with the maximum at -800 ppm does not narrow under MAS

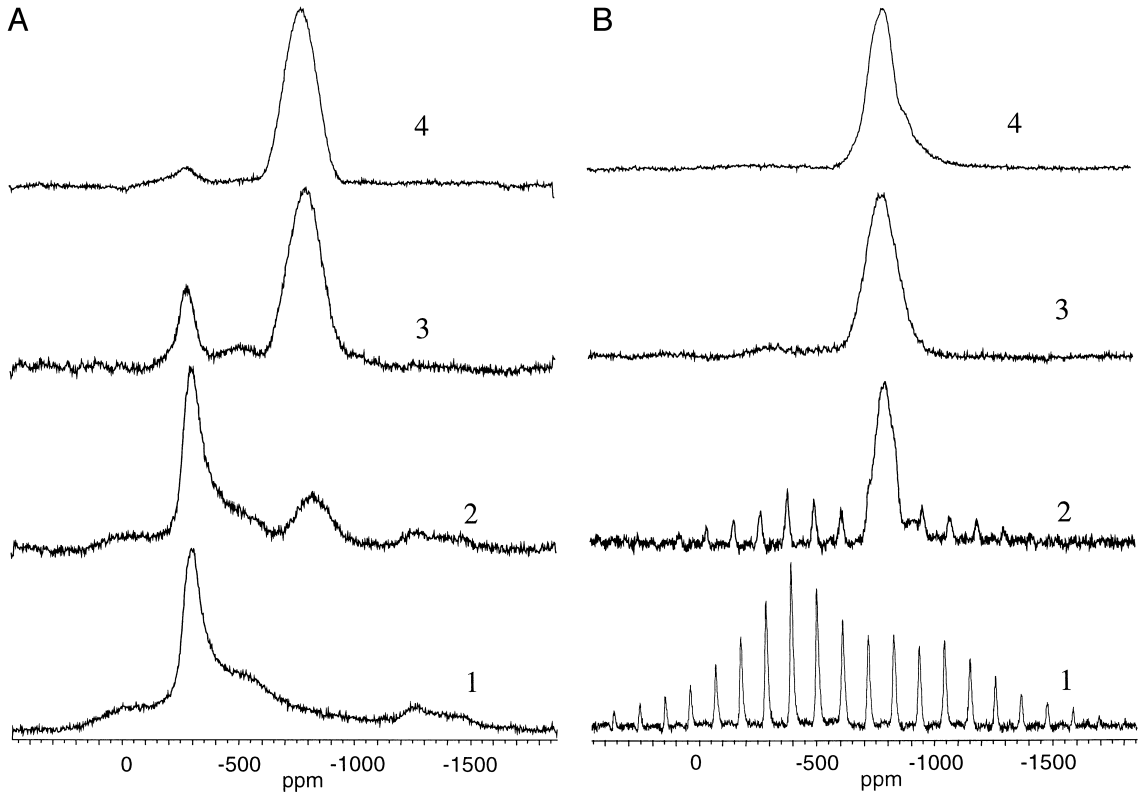

Fig. 2. The ^{51}V static (A) and MAS (B) spectra of VO_x/TiO_2 catalyst containing P_2O_5. (A) 3, 5, 10 and 15 wt.% of P_2O_5 (spectra 1, 2, 3, 4, respectively). (B) 1, 10 and 15 wt.% P_2O_5 (spectra 1, 2 and 3, respectively). Spectrum 4 was obtained after the extraction procedure of the soluble vanadium from the sample with initial P_2O_5 content of 15 wt.%.

conditions. One of the reasons of such behaviour may be related to the amorphous character of the catalysts. So, the actual identification of V–P compounds in this case could be successful only in case of the detailed knowledge of all NMR parameters for $VOPO_4$ phases, including the influence of some NMR parameters distribution on the resulted line shape.

Quantitative integration shows that up to 50% of the vanadium is not detected in the spectrum of catalysts with very low phosphorous contents and could be revealed only after acidic extraction of the excess of regular V_2O_5 as has been shown in Ref. [18] for pure VO_x/TiO_2 catalysts obtained by the spray-drying method. Based on the precise analysis of both static and MAS spectra [18], the authors have revealed a unique vanadium site with an extremely large quadrupole coupling constant (up to 15 MHz). This site is presumed to be the strongly bound vanadium (SBV) incorporated into the titania lattice with a significantly distorted octahedral oxygen environment. The introduction of phosphorous decreases the content of the SBV species, and in the catalysts with 15 wt.% of P_2O_5, SBV species were not detected after the extraction procedure (Fig. 2B-4). The ^{31}P and ^{51}V NMR spectra of the VO_x/TiO_2 (10 wt.% P_2O_5), after extraction of the soluble vanadium and phosphorous species, are almost the same as observed before the extraction (compare spectra 2,3 and 4 in Fig. 2B). The latter indicates that all vanadium atoms in the catalysts with high phosphorous concentrations are bound to phosphorous and that the compound formed is not soluble in the acidic solution.

There are several publications devoted to ^{31}P NMR spectra of $VOPO_4$ phases, whereas only Abde-

louahab et al. [15] published ^{51}V NMR spectra of (α_{II}-, β-, δ-, γ-) phases of $VOPO_4$. Unfortunately, neither chemical shielding tensor parameters nor quadrupole constants were determined in the above-mentioned paper. Moreover, authors have demonstrated only a small part (1/4) of both static and MAS spectra of $VOPO_4$ phases. The spectra with axial anisotropy of the chemical shielding tensor presented in this paper could be more or less useful for researcher, whereas the spectrum of α_{II}-$VOPO_4$ could only be imagined with the rich fantasy of the reader. That is why we have to determine the complete set of parameters of the chemical shielding and quadrupole tensors for the individual compounds, whose presence could not be excluded in our catalysts. Moreover, as it was mentioned in the introduction, the formation of (α_I-, α_{II}-, β-) $VOPO_4$ and $VOPO_4 \cdot 2H_2O$ was proposed by several authors for VO_x/TiO_2 catalysts promoted by phosphorous.

The $VOPO_4$ phases are composed of VO_6 octahedra and PO_4 tetrahedra [48–55]. The octahedra are distorted and exhibit a short vanadium–oxygen bond (V=O) and a long vanadium–oxygen bond (V−O). The other four oxygen atoms may be considered as equatorial atoms. The V−O equatorial bond length is intermediate between short and long bonds. The VO_6 octahedra in (α_I-, α_{II}-, β-) $VOPO_4$ phases form chains with alternating short and long vanadium–oxygen bonds. The VO_6 octahedra are linked to PO_4 tetrahedra in the direction perpendicular to the main chain direction.

The β-$VOPO_4$ phase differs from others by two oxygen atoms of each PO_4 tetrahedron shared with two octahedra belonging to the same chain, while the other two oxygen atoms of the PO_4 tetrahedron are shared with octahedra from different chains.

In (α_I-, α_{II}-) $VOPO_4$, oxygen atoms from any PO_4 tetrahedron are shared with octahedrons from different chains. The V–$O_{equatorial}$–P links are all identical for α_I-$VOPO_4$, while in β-$VOPO_4$, there are three different kinds of V–$O_{equatorial}$–P links with different angles. The main difference between α_I-$VOPO_4$ and α_{II}-$VOPO_4$ structures is the inversion in position of the vanadium and phosphorous atoms relative to the equatorial plane: V and P are on the same side for α_I-$VOPO_4$ and on the opposite sides for α_{II}-$VOPO_4$. The V=O short bond never intersects the equatorial plane.

The ^{51}V NMR parameters obtained in our experiments are in good agreement with the structural data for α_I-$VOPO_4$ and β-$VOPO_4$ mentioned above (Table 1, Figs. 3 and 4). Thus, the axial chemical shielding anisotropy observed for these compounds is typical for vanadium in distorted octahedral environments, with one short vanadium–oxygen bond. Large value of anisotropy indicates a very short

Table 1
^{51}V quadrupole tensor parameters (C_Q, η_Q)[a], chemical shielding tensor parameters (δ_σ, η_σ, σ_{iso})[b], and Euler angles (α, β, γ) describing the relative orientation of quadrupole tensor with respect to chemical shielding tensor for $VOPO_4$ from 105.25 MHz ^{51}V MAS and static NMR spectra

Data set	C_Q (kHz)	η_Q	δ_σ (ppm)	η_σ	σ_{iso} (ppm)[c]	σ_1 (ppm)[d]	σ_2 (ppm)[d]	σ_3 (ppm)[d]	α (degree)	β (degree)	γ (degree)
α_I-$VOPO_4$	1550	0.55	880	0.0	691	281	281	1511	54	163	–[e]
α_{II}-$VOPO_4$	825	0.52	582	0.67	776	287	680	1358	−7	0	−60
β-$VOPO_4$	1990	0.59	818	0.0	755	346	346	1573	6	43	–[e]

[a] Nuclear electric quadrupole moment eQ, electric field gradient tensor eigenvalues (V_1, V_2, and $V_3 = eq$) are connected with C_Q and η_Q by the relations: $C_Q = e^2qQ/h$; $V_1 = 1/2(-1 - \eta_Q)V_3$; $V_2 = 1/2(-1 + \eta_Q)V_3$.

[b] The eigenvalues of chemical shielding tensor are expressed by δ_σ, η_σ and σ_{iso} in the following manner: $\sigma_1 = 1/2\,\delta_\sigma(-1 - \eta_\sigma) + \sigma_{iso}$; $\sigma_2 = 1/2\,\delta_\sigma(-1 + \eta_\sigma) + \sigma_{iso}$; $\sigma_3 = \delta_\sigma + \sigma_{iso}$.

[c] σ_{iso} was determined from the position of the zero spinning sideband and presented here without second-order qudrupole shift correction which is small (about 0.1 ppm) as compared to experimental errors.

[d] σ_1, σ_2 and σ_3, computed from the values of δ_σ, η_σ, and σ_{iso} using the relations in table footnote b.

[e] Angles α and γ are determined with significant error because the symmetry of the chemical shielding tensor is close to axial, specially for γ, due to this, the value of γ is omitted.

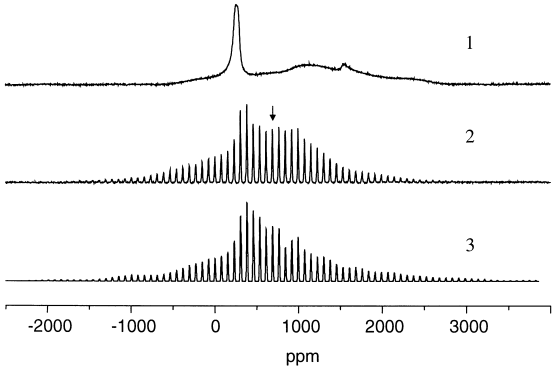

Fig. 3. Experimental static (spectrum 1) and MAS (spectrum 2) spectra ^{51}V NMR of the central and satellite transitions ($\nu_r = 8$ kHz) for α_I-$VOPO_4$. Spectrum 3 — simulated spectrum employs the optimised parameters from Table 1 and Gaussian broadening of 600 Hz. An arrow indicates the isotropic chemical shift.

V=O bond. The significant shift of the isotropic chemical shielding to higher fields up to 700–800 ppm results from the PO_4 surrounding the vanadium.

In contrast, the NMR parameters obtained for α_{II}-$VOPO_4$ are absolutely different (Table 1, Fig. 5). While for α_I-$VOPO_4$ and β-$VOPO_4$ phases, the ^{51}V chemical shielding tensors are close to axial; the chemical shielding tensor for α_{II}-$VOPO_4$ has three significantly different principal values. This difference may be due to a longer V=O bond in this compound. The latter could also be due to a smaller value of the anisotropy for α_{II}-$VOPO_4$ in comparison to α_I-$VOPO_4$ and β-$VOPO_4$ phases. According to the structural data for α_{II}-$VOPO_4$, all equatorial V–O bond lengths are very close (from 1.857 to 1.858 A). The short V=O bond is longer than in the other phases and has a length of 1.578 A. For example, in β-$VOPO_4$, the equatorial V–O bonds vary from 1.853 to 1.9023 A; the V=O bond is equal to 1.565 A. Different values of quadrupole constants in these phases are probably caused by the position of vanadium and phosphorous atoms close to the equatorial plane.

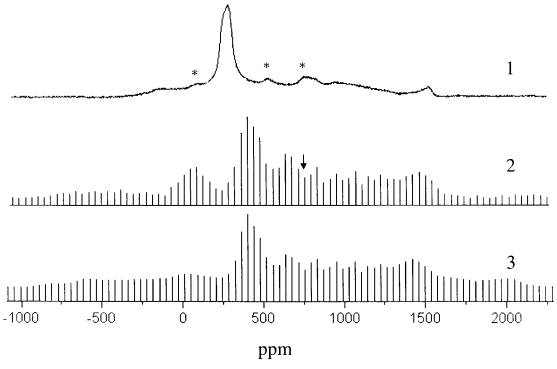

Fig. 4. Experimental static (spectrum 1) and MAS (stick plot spectrum 2) spectra ^{51}V NMR of the central and satellite transitions ($\nu_r = 5.9$ kHz) for β-$VOPO_4$. Spectrum 3 — simulated stick plot spectrum employs the optimised parameters from Table 1. An arrow indicates the isotropic chemical shift. An admixture of α_{II}-$VOPO_4$ in the static spectrum is indicated by asterisks.

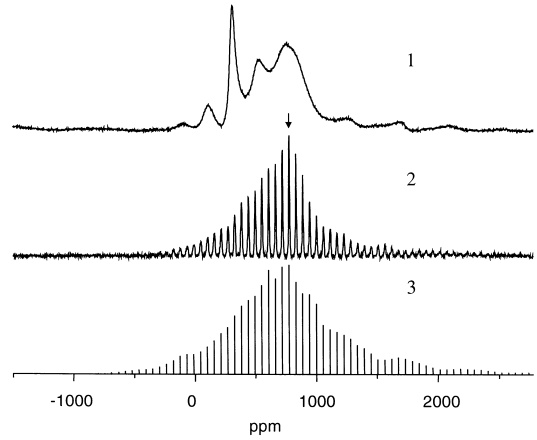

Fig. 5. Experimental static (spectrum 1) and MAS (spectrum 2) spectra ^{51}V NMR of the central and satellite transitions ($\nu_r = 5.9$ kHz) for α_{II}-$VOPO_4$. Spectrum 3 — simulated stick plot spectrum employs the optimised parameters from Table 1. The strong peak at −320 ppm in static spectra corresponds to partially hydrated $VOPO_4$, which does not narrow in MAS spectrum (the latter was exemplified in the text for $VOPO_4 \cdot 2H_2O$). An arrow indicates the isotropic chemical shift.

According to the literature data [43], the structure of $VOPO_4 \cdot 2H_2O$ resembles that of α-$VOPO_4$. The only difference is that the long V–O bonds in $VOPO_4 \cdot 2H_2O$ are replaced by V–OH_2 bonds, and there is no chain structure. This fact significantly influences the ^{51}V NMR spectra, which are significantly broadened by the exchange of H_2O molecules, and line narrowing is not observed in MAS experiments.

Based on both ^{51}V and ^{31}P NMR data, we may conclude that the $VOPO_4$ phase does not exist in the phosphorous-promoted VO_x/TiO_2 catalysts prepared by the spray-drying method. According to a small value of ^{51}V chemical shielding anisotropy,

vanadium atoms in these catalysts should be in slightly distorted tetrahedral coordination. The high value of the isotropic chemical shielding (800 ppm) unambiguously evidences that the vanadium atoms are bound to phosphorous via oxygen atoms. The single signal at -30 ppm in ^{31}P MAS spectra for the catalysts with different phosphorous concentrations indicates that all phosphorous atoms are bound to vanadium (according to ^{51}V NMR data, vanadium is bound to P), and that there is no phosphorous bound only to TiO_2 surface (as was proposed in the literature data). Nevertheless, taking into account the ability of phosphorous to easily interacts with both vanadium and titanium, one may suggest that in the promoted VO_x/TiO_2 catalysts, obtained by the spray-drying method, phosphorous is bound simultaneously to titanium and vanadium. There is another argument in favour of this suggestion. According to the data obtained by the Differential Dissolution technique [56], vanadium, phosphorous and titanium in these catalysts are dissolved simultaneously with a constant ratio close to 1:1:1. The latter could be only the case if an individual V–P–Ti compound is formed in these catalysts. The interaction between all the components in the system is favoured by the catalyst preparation procedure, according to which, an interaction of vanadium and phosphorous occurs with freshly precipitated sediment precursor of TiO_2, $Ti(OH)_4 \cdot nH_2O$, but not with crystalline TiO_2 usually used for catalyst preparation.

To clarify the structure of the formed V–P–Ti species, 2D 3QMAS and 5QMAS methods have been applied for the catalyst characterisation. The MQMAS experiments lead to a higher spectral resolution, as compared to that obtained in conventional MAS experiments. Moreover, MQMAS gives the possibility to determine the distribution of chemical shielding and quadrupole tensor parameters. The latter information is very important for the characterisation of the long-range environments of ^{51}V nuclei.

2D 3QMAS and 5QMAS spectra of V_2O_5/TiO_2 catalyst, containing 10% P_2O_5 are shown in Fig. 6. Two axes (F2 and F1) in these spectra correspond to the single-quantum (1Q) and triple-quantum (3Q) or quintuple-quantum (5Q) dimensions, respectively. The parts per million scales of the 2D spectrum are calculated with respect to ν_0 for the F2 dimension and $3\nu_0$ or $5\nu_0$ for the F1 dimension. The projection of the 2D spectrum on the F2 axis produces the conventional 1Q spectrum with some shape distortion due to imperfections in the rf pulses and in inter pulse delays.

According to these spectra, only one type of vanadium site is formed in the catalyst with an isotropic chemical shift near -755 ppm, with a very large distribution of quadropole constant (~ 7 MHz

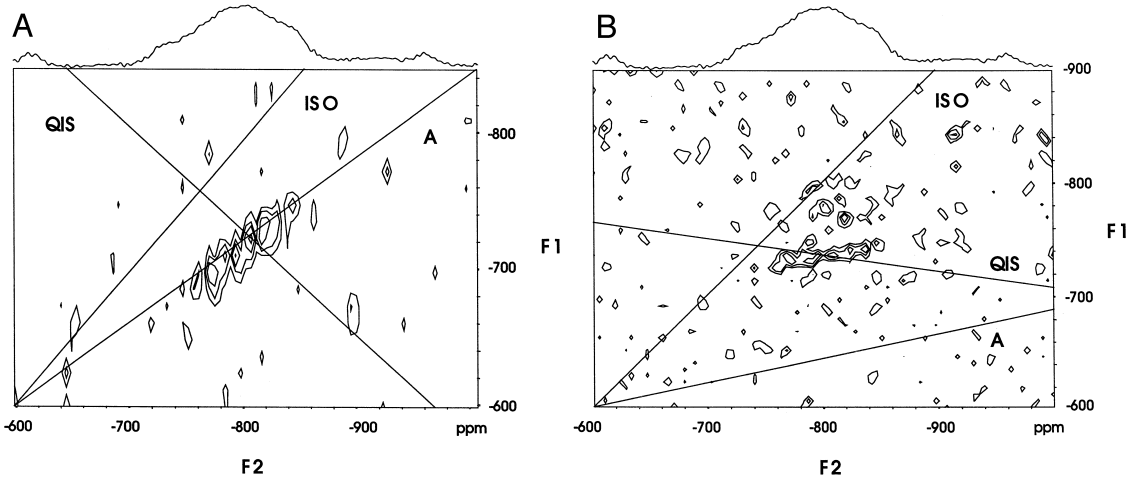

Fig. 6. 2D ^{51}V 3QMAS (A) and 5QMAS (B) spectra of VO_x/TiO_2 catalyst containing 10 wt.% P_2O_5. Isotropic (ISO), Anisotropic (A), Quadrupolar-Induced Shift (QIS) axes are marked.

in both directions) around its mean value of about 17 MHz. 5QMAS spectrum is more suitable for the discrimination between the quadrupole and chemical shielding parameter distributions than the 3QMAS spectrum. As could be seen from the 5QMAS spectrum, the distribution of quadrupole parameters significantly affects the observed spectrum, while the influence of chemical shielding distribution is less pronounced. According to this observation, we may conclude that the vanadium sites in the V–P–Ti compound formed are probably in slightly distorted tetrahedral coordination, whereas there are the strong distortions (different for each vanadium site) in the second coordination sphere. This points to the irregular structure of this compound.

4. Conclusion

Phosphorous-doped VO_x/TiO_2, catalysts prepared by the spray-drying method and treated under catalytic reaction, as well as individual phases (α_I-, α_{II}-, β-) of $VOPO_4$ were studied using modern high-resolution solid-state NMR techniques, including fast MAS, combined with the analysis of rotational satellites intensities by the SATRAS method; 2D triple-quantum, quintuple-quantum MAS NMR and spin mapping echo experiments. The simultaneous determination of chemical shielding anisotropy and quadrupole tensor parameters, as well as their distributions, permits to draw a conclusion on the local environment of vanadium sites in the catalysts. The formation of a triple V–P–Ti compound in phosphorous-doped VO_x/TiO_2 catalysts with the ratio of V:P:Ti close to 1:1:1 has been revealed. Only one type of slightly distorted tetrahedral vanadium atoms bound via oxygen to phosphorous was found in this compound. The very large distribution of quadrupole constant points to the irregular structure of this compound.

Acknowledgements

We are grateful to Dr. G.A.Zenkovets for the catalysts' preparation and to Prof. V.Malakhov for DD experiments. Partial support of this work by the Russian Foundation for Basic Research (project no. 98-03-32323), INTAS (project no. 97-0059) and NATO "Science for Peace" Program (Project number 971984) is acknowledged.

References

[1] Applied Catalysis A: General, 1997, 157
[2] G. Busca, L. Lietti, G. Ramis, F. Berti, Appl. Catal., B 18 (1998) 1.
[3] J. Soria, J.C. Conesa, M.L. Granados, R. Mariscal, J.L.G. Fierro, J.F. Garsia de la Banda, H. Heinemann, J. Catal. 120 (1989) 457.
[4] G. Deo, I.E. Wachs, J. Catal. 146 (1994) 335.
[5] A.J. van Hengstum, J. Pranger, J.G. van Ommen, P.J. Gellings, Appl. Catal. 11 (1984) 317.
[6] E.C. Alyea, L.J. Lakshmi, Z. Ju, Langmuir 13 (1997) 5621.
[7] R.A. Overbeek, P.A. Warringa, M.J.D. Crombag, L.M. Visser, A.J. van Dillen, J.W. Geus, Appl. Catal., A 135 (2) (1996) 209.
[8] J. El-Drissi, M. Kacimi, M. Loukah, M. Ziyad, J. Chim. Phys. Phys.-Chim. Biol. 94 (11/12) (1997) 1984.
[9] M. Ruitenbeek, A.J. VanDillen, D.C. Koningsberger, J.W. Geus, Stud. Surf. Sci. Catal. 118 (1998) 549, (Preparation of Catalysts VII).
[10] J. Li, M.E. Lashier, G.L. Schrader, B.C. Gerstei, Appl. Catal. 73 (1991) 83.
[11] M.T. Sananes, A. Tuel, J.C. Volta, J. Catal. 145 (1994) 251.
[12] M.T. Sananes, A. Tuel, G.J. Hutchings, J.C. Volta, J. Catal. 148 (1994) 395.
[13] M. Abon, K.E. Bere, A. Tuel, P. Delichere, J. Catal. 156 (1995) 28.
[14] V.V. Guliants, J.B. Benziger, S. Sundaresan, I.E. Wachs, J.M. Jehng, J.E. Roberts, Catal. Today 28 (1996) 275.
[15] F.B. Abdelouahab, R. Olier, N. Guilhaume, F. Lefebre, J.C. Volta, J. Catal. 134 (1992) 151.
[16] K. Ait-Lachgar, A. Tuel, J.M. Herrmann, J.M. Krafft, J.R. Martin, J.C. Volta, M. Abon, J. Catal. 177 (1998) 224.
[17] J.C. Vedrine, J.M.M. Millet, J.C. Volta, Faraday Discuss. Chem. Soc. 87 (1989) 207.
[18] A. Shubin, O.B. Lapina, V.M. Bondareva, Chem. Phys. Lett. 302 (1999) 341.
[19] O.B. Lapina, A.V. Simakov, V.M. Mastikhin, S.A. Veniaminov, A.A. Shubin, J. Mol. Catal. 50 (1989) 55.
[20] H. Eckert, I. Wachs, J. Phys. Chem. 93 (1989) 6796.
[21] O.B. Lapina, V.M. Mastikhin, A.A. Shubin, V.V. Krasilnikov, K.I. Zamaraev, Prog. Nucl. Magn. Reson. Spectrosc. 24 (1992) 457.
[22] V.M. Mastikhin, O.B. Lapina, Vanadium catalysts: solid-state NMR, NMR Encyclopedia vol. 8, 1996, p. 10771.
[23] O.B. Lapina, A.A. Shubin, A.V. Nosov, E. Bosch, J. Spenler, H. Knözinger, J. Phys. Chem. 103 (1999) 7599.
[24] J. Skibsted, N.C. Nielsen, H. Bildsøe, H.J. Jakobsen, Chem. Phys. Lett. 188 (1992) 405.

[25] J. Skibsted, N.C. Nielsen, H. Bildsøe, H.J. Jakobsen, J. Am. Chem. Soc. 115 (1993) 7351.
[26] C. Jäger, NMR Basic Princ. Prog. 31 (1994) 133.
[27] C. Fernandez, P. Bodart, J.P. Amoureux, Solid-State NMR 3 (1994) 79.
[28] J. Skibsted, T. Vosegaard, H. Bildsøe, H. Jakobsen, J. Am. Chem. Soc. 100 (1996) 14872.
[29] J. Skibsted, C.J.H. Jacobsen, H.J. Jakobsen, Inorg. Chem. 37 (1998) 3083.
[30] J.P. Amoureux, C. Fernandez, L. Carpentier, E. Cochon, Phys. Status Solidi A 132 (1992) 461.
[31] L. Frydman, J.S. Harwood, J. Am. Chem. Soc. 117 (1995) 5367.
[32] A. Medek, J.S. Harwood, L. Frydman, J. Am. Chem. Soc. 117 (1995) 12779.
[33] J.-P. Amoureux, C. Fernandez, L. Frydman, Chem. Phys. Lett. 259 (1996) 347.
[34] D. Massiot, B. Touzo, D. Trumeau, J.P. Coutures, J. Virlet, P. Florian, P.J. Grandinetti, Solid-State NMR 6 (1996) 73.
[35] S.P. Brown, S.J. Heyes, S. Wimperis, J. Magn. Reson., Ser. A 119 (1996) 280.
[36] S.H. Wang, Z. Xu, J.H. Baltisberger, L.M. Bull, J.F. Stebbins, A. Pines, Solid-State NMR 8 (1997) 1.
[37] A.P.M. Kentgens, Geoderma 80 (1997) 271.
[38] J.P. Amoureux, C. Fernandez, Solid-State NMR 10 (1998) 211.
[39] T. Charpeutier, J. Virlet, Solid-State NMR 12 (1998) 227.
[40] G. Ladwig, Z. Anorg. Chem. 338 (1965) 266.
[41] E. Bordes, P. Courtine, G. Pannetier, Ann. Chim. 8 (1973) 105.
[42] E. Bordes, P. Courtine, J. Catal. 57 (1979) 236.
[43] H.R. Tietze, Aust. J. Chem. 34 (1965) 266.
[44] G.N. Kryukova, D.O. Klenov, G.A. Zenkovets, React. Kinet. Catal. Lett. 60 (1997) 179.
[45] A.A. Shubin, O.B. Lapina, G.M. Zhidomirov, IXth AMPERE Summer School, Abstracts, Novosibirsk, USSR, 20–26 Sept. 1987, p. 103.
[46] A.A. Shubin, O.B. Lapina, D. Courcot, Catal. Today 56 (2000) 379, (contributors: A.A. Shubin, O.B. Lapina, D. Courcot, A. Aboukais, B. Revel, M. Rigole, M. Guelton, S. Caldarelli, J.C. Vedrine).
[47] A.A. Shubin, O.B. Lapina, E. Bosch, H. Knözinger, J. Phys. Chem. 103 (1999) 3138.
[48] E. Bordes, Catal. Today 1 (1987) 499.
[49] E. Bordes, P. Courtine, J.W. Johnson, J. Solid-State Chem. 55 (1984) 270.
[50] G.Z. Ladwig, Z. Anorg. Chem. 338 (1965) 266.
[51] R. Gopal, C. Calvo, J. Solid-State Chem. 5 (1972) 432.
[52] F.B. Abdelouahab, R. Olier, N. Guilhaume, F. Lefebre, J.C. Volta, J. Catal. 134 (1992) 151.
[53] B. Jordan, C. Calvo, Can. J. Chem. 51 (1973) 2621.
[54] E. Bordes, J.W. Johnson, A. Raminosova, P. Courtine, Mater. Sci. Monogr. 28B (1985) 887.
[55] T.P. Mozer, G.L. Schrader, J. Catal. 92 (1985) 216.
[56] V.V. Malakhov, A.A. Vlasov, Kinet. Katal. 36 (1995) 503.